JOURNAL OF GUIDANCE, CONTROL, AND DYNAMICS
Vol. 25, No. 5, September–October 2002

Multivariable Adaptive Control Design with Applications to Autonomous Helicopters

A. S. Krupadanam
Maxtor Corporation, Shrewsbury, Massachusetts 01545
A. M. Annaswamy
Massachusetts Institute of Technology, Cambridge, Massachusetts 02139
and
R. S. Mangoubi
Charles Stark Draper Laboratory, Inc., Cambridge, Massachusetts 02139

Control of autonomous helicopters in the presence of environmental and system uncertainties is a challenging task. These uncertainties not only change the dynamics of the system but the trim inputs themselves. A viable multivariable adaptive control methodology is proposed that is applicable for general maneuvers with arbitrary speeds and high-bandwidth requirements. The control design methodology achieves global stability and is tested on a high-fidelity simulation of a real life autonomous helicopter. The results indicate a satisfactory tracking performance even as the speeds and bandwidth requirements are increased well beyond hover and as the parametric uncertainties were increased by about 20% of their nominal values.

A. S. Krupadanam received his B.Tech (B.S. equivalent) degree in mechanical engineering from the Indian Institute of Technology, Kharagpur, in 1995 and an M.S. in mechanical engineering from Boston University in 1996, where he was a Presidential University Graduate Fellow. He received his Ph.D. in mechanical engineering from the Massachusetts Institute of Technology in 2001. He is currently working as a Staff Engineer at Maxtor Corp., Shrewsbury, Massachusetts, e-mail at krupa@alum.mit.edu. His research interests include adaptive, nonlinear, and robust control, and control applications in aerospace, disk drive, and thermofluid systems.

A. M. Annaswamy received her Ph.D. degree in electrical engineering from Yale University in 1985. She has been a member of the faculty at Yale, Boston University, and the Massachusetts Institute of Technology, where currently she is the director of the Active-Adaptive Control Laboratory and a Principal Research Scientist in the Department of Mechanical Engineering, e-mail at aanna@mit.edu. Her research interests pertain to adaptive control, active control of resonant thermofluid systems including combustion processes and supersonic flows, and neural networks. She has authored numerous journal and conference papers and coauthored a graduate textbook on adaptive control. A. M. Annaswamy has received several awards including the Alfred Hay Medal from the Indian Institute of Science in 1977, the Stennard Fellowship from Yale University in 1980, the IBM postdoctoral fellowship in 1985, the George Axelby Outstanding Paper award from the Institute of Electrical and Electronics Engineers Control Systems Society in 1988, and the Presidential Young Investigator award from the National Science Foundation in 1991. A. M. Annaswamy is a Member of AIAA.

R. S. Mangoubi received his doctorate in estimation and control from the Massachusetts Institute of Technology Aeronautics and Astronautics Department in 1995. He has been a member of the technical staff at Charles Stark Draper Laboratory, Inc., Cambridge, Massachusetts, since 1983, where he is currently in the Autonomous Control group, e-mail at rmangoubi@draper.com. Throughout his career, he worked on problems and led projects in the areas of operations research, control, and statistical signal detection, with a wide range of applications including computer networks, biochemical sensing, magnetic resonance brain imaging, and control of and detection of failures in autonomous and space vehicles. Earlier in his career, he introduced the use of robust game theoretic filters for failure detection in dynamic plants. His current research activities include work in the areas of robust non-Gaussian signal detection, ad hoc communication, and the application of combustion control to space engines. R. S. Mangoubi is the author of numerous publications, including *Robust Estimation and Failure Detection: A Concise Treatment*, published by Springer-Verlag. He supervises graduate students conducting their research at Draper Laboratory. He was an invited plenary speaker for the *2000 International Federation of Automatic Control* (IFAC) SAFEPROCESS conference in Budapest, Hungary. He is also a member of the IFAC SAFEPROCESS Technical Committee, and a Senior Member of AIAA.

Received 5 November 2001; revision received 11 May 2002; accepted for publication 15 May 2002.

Nomenclature

A	=	state-space representation matrix
A_p	=	state-space representation matrix about nominal trim
$a_{\mathrm{FB}}, a_{\mathrm{mr}}, a_{\mathrm{tr}}$	=	lift curve slope of flybar, main rotor blade, and tail rotor blade, respectively
a_1	=	rotor disk pitch angle
$a_{1,\mathrm{FB}}$	=	flybar pitch angle
B	=	state-space representation matrix
B_m	=	reference model state space representation matrix
B_p	=	state-space representation matrix about nominal trim
$b_{\mathrm{mr}}, b_{\mathrm{tr}}$	=	number of main rotor blades and tail rotor blades, respectively
b_1	=	rotor disk roll angle
$b_{1,\mathrm{FB}}$	=	flybar roll angle
C	=	state space representation matrix
$C_{D0,\mathrm{mr}}, C_{D0,\mathrm{tr}}$	=	zero-lift drag coefficient of main rotor blade and tail rotor blade, respectively
C_i	=	controller parameter matrix of size $m \times m, i = 1, \ldots, \nu - 1$
$c_{\mathrm{FB}}, c_{\mathrm{mr}}, c_{\mathrm{tr}}$	=	chord of flybar paddle, main rotor blade, and rotor blade, respectively
D_e	=	gear reduction ratio of main rotor
D_j	=	controller parameter matrix of size $m \times m, j = 0, \ldots, \nu - 1$
D_{tr}	=	tail rotor turns per turn of main rotor
d_x, d_y	=	state and output disturbance, respectively
d_0	=	input disturbance due to d_x and d_y
d_1	=	output disturbance
$\hat{d}$	=	trim error estimate
e	=	state error $x_p - x_m$
e_0, e_1, e_2, e_3	=	quaternion element
$e_1(t)$	=	output error $z_p(t) - z_m(t)$
f	=	system dynamics
g	=	gravitational acceleration
$H_p(s)$	=	Hermite normal form of system transfer function matrix
I_b, I_{FB}	=	flapping inertia of main rotor blade and flybar paddle, respectively
I_{xx}, I_{yy}, I_{zz}	=	roll axis, pitch axis, and yaw axis moment of inertia, respectively
K	=	control matrix
$K_{\mathrm{cyc}}^{\mathrm{fb}}$	=	flybar cyclic pitch per cyclic pitch control input
$K_{\mathrm{fb}}^{\mathrm{cyc}}$	=	main rotor cyclic pitch per flybar tip path deflection
K_{GE}	=	ground effect parameter
K_p	=	high-frequency gain of $W_p(s)$
$K_0, \bar{K}_0$	=	controller parameter matrix of size $m \times m$
$\bar{K}_p$	=	high frequency gain of plant with precompensator
k_i	=	measure of column relative degree
m	=	number of input and outputs of $W_m(s)$
m_e	=	mass without fuel
m_f	=	fuel capacity
$\dot{m}_{\max}$	=	fuel consumption rate at maximum output
n	=	order of plant
n_i^*	=	relative degree of individual elements of $W_p(s)$
P	=	adaptation gain matrix
P_{bhp}	=	engine brake power
p	=	body roll rate
Q	=	control matrix
Q_0	=	positive definite matrix
q	=	body pitch rate
R_{FB}	=	radius of center of flybar paddle
R_{mr}	=	main rotor radius
$R_m(s)$	=	polynomial matrix of monic Hurwitz polynomials
$R_p(s)$	=	polynomial matrix in coprime matrix fraction decomposition of $W_p(s)$
$R_{p_{\mathrm{ad}}}(s)$	=	adjoint of $R_p(s)$
$R_{p_{\mathrm{rc}}}$	=	matrix column form of $R_p(s)$
$R_q(s)$	=	diagonal matrix of polynomial transfer functions
R_{tr}	=	tail rotor radius
r	=	body yaw rate
r_m	=	reference input
$r_q(s)$	=	Hurwitz monic polynomial of degree $\nu - 1$
S_a, S_{ld}, S_{li}	=	selector matrix
s_{FB}	=	span of flybar paddle
T	=	postcompensator matrix
T_i	=	nonsingular matrices made of unit vectors, $i = 1, 2$
U	=	system input
$U_{\mathrm{col}}, U_{\mathrm{pcyc}}, U_{\mathrm{rcyc}}$	=	main rotor collective, pitch cyclic, and roll cyclic
U_e	=	trim input to plant
U_g	=	forward velocity (ground frame), ft/s
U_{ped}	=	tail rotor collective
U_{thr}	=	engine throttle
U_0	=	nominal trim input to plant
U_0^*	=	searched nominal trim input
U_1	=	intermediate nominal trim input during search
u	=	forward velocity (body frame), ft/s
u_p	=	system input linearized about nominal trim
u_{pe}	=	system input linearized about trim
V_w	=	wind velocity vector (local-level frame)
v	=	lateral velocity (body frame), ft/s
v_p	=	input with precompensation
$W_a(s)$	=	gradient stabilizer transfer function matrix
$W_c(s)$	=	precompensator transfer matrix
$W_{\mathrm{cl}}(s)$	=	closed-loop transfer function matrix
W_g	=	vertical velocity (ground frame), ft/s
$W_m(s)$	=	reference model transfer function matrix
$W_p(s)$	=	plant transfer function matrix
$\bar{W}_p(s)$	=	plant with precompensator
w	=	vertical velocity (body frame), ft/s
X	=	system state
X_a	=	fixed part of nominal trim
X_b	=	part of nominal trim determined through search
$X_c, \dot{X}_c$	=	commanded state and commanded state derivative, respectively
X_{c_1}, X_{c_2}	=	part of commanded state
$\dot{X}_{c_3}, \dot{X}_{c_4}$	=	part of commanded state derivative
X_e	=	trim state of plant
$\dot{X}_e$	=	commanded state derivative for trim
X_g	=	north position (ground frame), ft
$X_{uu,\mathrm{fus}}$	=	axial fuselage drag coefficient
X_0	=	nominal trim state of plant
X_{0_1}, X_{0_2}	=	part of nominal trim state
$\dot{X}_{0_3}, \dot{X}_{0_4}$	=	part of nominal trim state derivative
X_0^*	=	searched nominal trim state
$\dot{X}_0$	=	commanded state derivative for nominal trim
X_1	=	intermediate nominal trim state during search
x	=	north position (local-level frame), ft
x_{ht}	=	horizontal tail c.p. location (forward of c.g.)
x_m	=	reference model state
x_{mr}	=	main rotor hub location (forward of c.g.)
x_p	=	system state linearized about nominal trim
x_{pe}	=	system state linearized about trim
x_{tr}	=	tail rotor hub location (forward of c.g.)
x_{vt}	=	vertical tail c.p. location (forward of c.g.)
Y	=	system output
Y_c	=	commanded output
Y_g	=	east position (ground frame), ft
$Y_{uu,\mathrm{vt}}$	=	trim vertical tail lift coefficient
$Y_{uv,\mathrm{ht}}$	=	vertical tail lift coefficient due to sideslip angle
$Y_{VV,\mathrm{vt,max}}$	=	maximum vertical tail lift coefficient
$Y_{vv,\mathrm{fus}}$	=	lateral fuselage drag coefficient
$Y_{vv,\mathrm{ht}}$	=	vertical tail lift coefficient due to sidewash
y	=	east position (local-level frame), ft
y_c	=	commanded output linearized about nominal trim

y_{pe} = system output linearized about trim
$Z_c(s)$, $Z_d(s)$ = controller polynomial matrix
$Z_p(s)$ = polynomial matrix in coprime matrix fraction decomposition of $W_p(s)$
$Z_{uu,\mathrm{ht}}$ = trim horizontal tail lift coefficient
$Z_{uw,\mathrm{ht}}$ = horizontal tail lift coefficient due to angle of attack
$Z_{VV,\mathrm{ht,max}}$ = maximum horizontal tail lift coefficient
$Z_{ww,\mathrm{fus}}$ = vertical fuselage drag coefficient
$Z_{ww,\mathrm{ht}}$ = horizontal tail lift coefficient due to downwash
z = down position (local-level frame), ft
z_{fus}, z_{ht} = fuselage and horizontal tail c.p. location (below c.g.), respectively
z_m, z_p = modified reference and modified plant output, respectively
z_{mr}, z_{tr} = main rotor and tail rotor hub location (below c.g.), respectively
z_{vt} = vertical tail c.p. location (below c.g.)
Γ = inverse of adaptation gain matrix
Γ_{r1}, Γ_{r2}, Γ_{r3} = adaptation robustness gain, Γ_r/s
Γ_1, Γ_2, Γ_3 = adaptation gain
η = efficiency of engine
$\boldsymbol{\Theta}$ = system parameter vector
Θ_c = controller parameter matrix
Θ_s = set of all system parameter values
$\bar{\Theta}_c$ = augmented controller parameter matrix
$\bar{\Theta}_c^*$ = ideal controller parameter matrix
$\boldsymbol{\Theta}_0$ = nominal system parameter vector
θ = pitch attitude
λ_f = fraction of fuel capacity remaining
ν = observability index of plant
π_p = monic polynomial of degree 1
ρ = atmospheric density
$\Phi(t)$ = controller parameter error matrix
ϕ = roll attitude
ψ = heading angle
Ω = angular rate of main rotor
$\Omega_{\max}$ = engine speed at maximum output
ω = nonminimal representation of x_p
ω_i, ω_j = part of nonminimal state ω, $i = 1, \ldots, \nu - 1$ and $j = \nu, \ldots, 2\nu - 1$, respectively
$\bar{\omega}$ = augmented nonminimal state representation
$\boldsymbol{\omega}_0$ = vector of unit elements

I. Introduction

THE control problem of high-performance helicopters is a challenging task because the vehicle dynamics are highly nonlinear and fully coupled, (Fig. 1) (Ref. 1) and subject to parametric uncertainties. Often, during complex maneuvers, the thrust is a function of roll, pitch, and heading angles. Control inputs are invariably limited to variations in pitch of main rotor and tail rotor blades and the throttle. In addition, the tail rotor needs to cancel out exactly the rotational torque due to the main rotor for the helicopter to maintain steady yaw angle. Some of the system parameters can change with the environment, for example, the aerodynamic constants, or with the helicopter, for example, lift curve slopes. The unknown system parameters also cause the trim conditions for the helicopter to be unknown. The complexity of this problem remains just as high in the case of both unmanned helicopters, where remote communications with the ground are used for control, as well as autonomous helicopters, where it is expected that little or no information from the ground is utilized for control. In this paper, our focus is on the latter for which we develop an adaptive multivariable controller that is capable of simultaneously accommodating all coupling features, parametric uncertainties, and the trim error and, as a result, executes complex maneuvers autonomously.

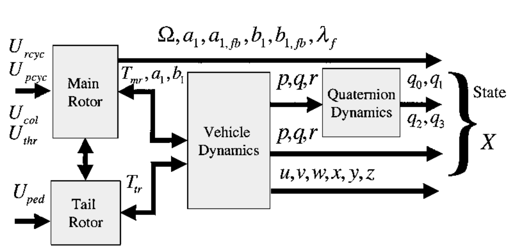

Fig. 1 Schematic of helicopter dynamics.

Great strides have been made in unmanned helicopter technology in the past few decades. Controller designs for these vehicles have involved highly augmented controller structures.[2–5] These controllers have multiple–inputs and multiple–outputs, are robust, and have enabled aggressive flight performance while ensuring stability. Typically, in such vehicles, remote communications are maintained with a ground station for obtaining ground-based reference signals, which are in turn used to compute the desired control inputs. In contrast, in an autonomous helicopter, the controller has to generate the appropriate action without these reference signals and still deliver the requisite high performance. A direct consequence of this is the introduction of an unknown trim error, which can be eliminated by a pilot and a ground station in a manned and unmanned helicopter, respectively. This problem is further exacerbated in the context of system uncertainties, which introduce an additional unknown component into the trim error as the trim commands change with the uncertainties. Although the incorporation of integrals can help mitigate this problem, it is often at the expense of trading off performance. What is more desirable is a control methodology that is capable of adapting to the trim error while simultaneously accommodating all coupling features and parametric uncertainties during the execution of maneuvers.

Previous work on linear control design for helicopters includes the use of eigenstructure assignment,[6–8] H_2, H_∞(Ref. 9), μ-synthesis,[10,11] and dynamic inversion methods.[12] These methods are based on linearized helicopter models about hover, uniform forward flight trim conditions, or the assumption that the modes are decoupled. Nonlinear control designs previously attempted include neural-network-based controllers,[13] fuzzy control,[14,15] differential flatness,[16] and backstepping designs.[17] These methods either assume feedback linearizability, which in turn restricts the motion to be around hover, or do not include parametric uncertainties, or realistic aerodynamics. Specific issues such as unknown trim conditions that degrade the performance of the helicopter have not been addressed. Whereas adaptive control schemes have been proposed in the aircraft and spacecraft control context,[18] there is a lack of similar work on helicopter control. The nonminimum phase nature of the helicopter dynamics adds to the challenge of finding a stable adaptive controller.

In this paper, our objective is to present an adaptive controller that addresses the special needs of autonomous vehicles. The proposed multivariable adaptive controller comprises the following features: It accommodates both parametric and unknown trim conditions through online adjustments of parameters. Suitable Lyapunov functions ensure closed-loop stability and robustness. The control design judiciously integrates linear design with online adaptive strategies, to maximize benefit from offline information and online measurements. A two-step nonlinear optimization procedure is carried out to determine nominal trim states that allows the arbitrarily close convergence to the global minima by making use of prior information available about sub-components of the trim states during a given maneuver. The performance of the controller is demonstrated using a high-fidelity nonlinear simulation model of Charles Stark Draper Laboratory's autonomous helicopter.

The new control design structure, together with a trim error estimate, controller parameter update laws, and system augmentation for stable adaptation, leads to a stable robust system with enhanced performance, thereby resulting in a viable multivariable adaptive controller for helicopters. Overall, the suggested design methodology reduces the gap between state-of-the-art adaptive control theory and design for non-full-state feedback systems and the needs of realistic applications such as autonomous helicopters.

The paper is organized as follows. In Sec. II, the problem is stated and a brief description of the nonlinear model of the helicopter dynamics used in Sec. III is presented. In Sec. III, the adaptive control design methodology is presented. Section IV compares the performance of the adaptive controller with that of other controllers using different scenarios, and Sec. V. offers conclusions.

II. Statement of the Problem

In this section, a statement of the problem and the helicopter model used for the design of the adaptive controller is described (Sec. II.A). The unknown trim conditions are then described (Sec. II.B) followed by a description of the effect of using a nominal trim (Sec. II.C).

A. Control Problem

Our goal is to design controllers for autonomous helicopters so that accurate command following is achieved. A helicopter dynamics model developed at Charles Stark Draper Laboratory[1,19–21] is used to develop the control design. This model is obtained by considering the fuselage of the helicopter as a rigid body attached to the main rotor and tail rotor. The six-degree-of-freedom equations of the fuselage are derived from Newton's second law.

The system can be expressed as an equivalent block f in the following manner:

$$\dot{X} = f(X, U, \mathbf{\Theta}) \tag{1}$$

For the helicopter,

$$X = [e_0, e_1, e_2, e_3, u, v, w, p, q, r, x, y, z, \Omega, a_1, b_1, a_{1,\mathrm{FB}}, b_{1,\mathrm{FB}}, \lambda_f]^T \tag{2}$$

$$U = [U_{\mathrm{rcyc}}, U_{\mathrm{pcyc}}, U_{\mathrm{ped}}, U_{\mathrm{col}}, U_{\mathrm{thr}}]^T \tag{3}$$

$$\begin{aligned}\mathbf{\Theta} = \big[&m_e, m_f, g, I_{xx}, I_{yy}, I_{zz}, x_{\mathrm{mr}}, z_{\mathrm{mr}}, R_{\mathrm{mr}}, a_{\mathrm{mr}}, b_{\mathrm{mr}}, c_{\mathrm{mr}}, C_{D0,\mathrm{mr}},\\ &I_b, K_{\mathrm{GE}}, R_{\mathrm{FB}}, a_{\mathrm{FB}}, c_{\mathrm{FB}}, s_{\mathrm{FB}}, I_{\mathrm{FB}}, K_{\mathrm{cyc}}^{\mathrm{fb}}, K_{\mathrm{fb}}^{\mathrm{cyc}}, \rho, x_{\mathrm{tr}}, z_{\mathrm{tr}},\\ &D_{\mathrm{tr}}, R_{\mathrm{tr}}, a_{\mathrm{tr}}, b_{\mathrm{tr}}, c_{\mathrm{tr}}, C_{D0,\mathrm{tr}}, P_{\mathrm{bhp}}, \eta, \Omega_{\max}, \dot{m}_{\max}, D_e, z_{\mathrm{fus}},\\ &X_{uu,\mathrm{fus}}, Y_{vv,\mathrm{fus}}, Z_{ww,\mathrm{fus}}, x_{\mathrm{ht}}, z_{\mathrm{ht}}, Z_{uu,\mathrm{ht}}, Z_{uw,\mathrm{ht}}, Z_{ww,\mathrm{ht}}\\ &Z_{VV,\mathrm{ht,max}}, x_{\mathrm{vt}}, z_{\mathrm{vt}}, Y_{uu,\mathrm{vt}}, Y_{uv,\mathrm{vt}}, Y_{vv,\mathrm{vt}}, Y_{VV,\mathrm{vt,max}}\big]\end{aligned} \tag{4}$$

Of the state variables in X, here a_1, b_1, $a_{1,\mathrm{FB}}$, $b_{1,\mathrm{FB}}$, and λ_f are difficult and expensive to measure and are, therefore, not available in most cases. Similarly, an exact measure of λ_f is also usually not available. Therefore, the system output is given by

$$Y = [e_0, e_1, e_2, e_3, u, v, w, p, q, r, x, y, z, \Omega] \tag{5}$$

In terms of the vehicle model described in Eqs. (1–5), the problem under consideration can, therefore, be stated as follows. For the system given by Eqs. (1–5), the objective is to find U such that $Y \to Y_c$ while all other signals remain bounded in the presence of uncertainties in the helicopter and environment, for any given operating condition.

B. Effect of Unknown Trim Conditions

One of the most common methods of controlling the nonlinear system in Eq. (1) is through linearization. The linearized model corresponding to Eq. (1) is given by

$$\dot{x}_{pe} = Ax_{pe} + Bu_{pe}, \qquad y_{pe} = Cx \tag{6}$$

where

$$x_{pe} = X - X_e, \qquad u_{pe} = U - U_e, \qquad y_{pe} = Y - CX_e \tag{7}$$

Suppose the goal is to carry out a forward flight or a vertical climb. X_e and U_e must satisfy the equation

$$f(X_e, U_e, \mathbf{\Theta}) = 0 \tag{8}$$

The determination of trim conditions for a given maneuver is tantamount to finding solutions of a set of nonlinear equations as in Eq. (8). This determination becomes even more complex in the presence of uncertainties. This is because $\mathbf{\Theta}$ in Eq. (8) is unknown, and, therefore, the trim conditions X_e and U_e, which are obtained as solutions of Eq. (8), are unknown as well. As a result, x_{pe}, u_{pe}, and y_{pe} in Eq. (7) are not measurable. Therefore, even the very first step in the control design cannot be taken due to the presence of uncertainties.

One possible approach for overcoming this difficulty is to estimate $\mathbf{\Theta}$ at a simple maneuver, such as the hover, using parameter identification methods, and proceed to determine X_e and U_e and, therefore, the linear controller using Eq. (6). However, because environmental and system conditions change during the vehicle maneuvers, new changes in $\mathbf{\Theta}$ can occur. These in turn necessitate continued estimation of either $\mathbf{\Theta}$ or its effects on the trim conditions. We adopt such an approach in this paper of an adaptive control design where the unknown trim condition is estimated online in addition to the estimation of the control parameters, to generate the desired control input.

C. Nominal Trim Condition

Because pilot action to achieve the trim conditions in flight, $X_e(\mathbf{\Theta})$ and $U_e(\mathbf{\Theta})$, is not available in the case of an autonomous helicopter, we choose a pseudotrim condition, X_0 and U_0, for a known nominal value $\mathbf{\Theta}_0$, of $\mathbf{\Theta}$. Thus,

$$X_0 = X_e(\mathbf{\Theta}_0) \tag{9}$$

$$U_0 = U_e(\mathbf{\Theta}_0) \tag{10}$$

Linearizing the plant in Eq. (1) about X_0 and U_0 for simple maneuvers that satisfy Eq. (8), we obtain that

$$\begin{aligned}\dot{x}_p &= A_p(\mathbf{\Theta})x_p + B_p(\mathbf{\Theta})u_p + d_x(\mathbf{\Theta})\\ y_p &= Cx_p + d_y(\mathbf{\Theta})\end{aligned} \tag{11}$$

$$\begin{aligned}d_x(\mathbf{\Theta}) &= A_p(\mathbf{\Theta})(X_0 - X_e) + B_p(\mathbf{\Theta})(U_0 - U_e)\\ d_y(\mathbf{\Theta}) &= C(X_0 - X_e)\end{aligned} \tag{12}$$

where $x_p = X - X_0$, $u_p = U - U_0$, and $\dot{x}_p = \dot{X} - \dot{X}_0$. It can be seen from Eq. (12) that unknown constant disturbances $d_x(\Theta)$ and $d_y(\Theta)$ are now added because of the unknown trim conditions. The matrices $A_p(\Theta)$ and $B_p(\Theta)$ are also affected by parametric uncertainties. An adaptive controller, to accommodate the parametric uncertainties and to compensate for the unknown trim, is, therefore, considered for control of this system. The objective is to design a u_p such that y_p follows y_c, where

$$y_c = Y_c - CX_0 \tag{13}$$

The earlier problem statement becomes more complex in the context of a complex maneuver. In such a case, unlike Eq. (8), given X_c, X_0, and U_0, satisfy the equation

$$f(X_e, U_e, \Theta) = \dot{X}_c \tag{14}$$

where $\dot{X}_c$ is not only nonzero but only partially specified. For example, in a coordinated turn, for a specified u and Ψ, p is known to be zero, but ϕ is to be determined; θ is zero (or a small value) but q needs to be calculated. In such cases, the solutions X_e and U_e need to be found using the following procedure: Let

$$X_0 = T_1\begin{bmatrix} X_{0_1}\\ X_{0_2}\end{bmatrix}, \qquad \dot{X}_0 = T_2\begin{bmatrix} \dot{X}_{0_3}\\ \dot{X}_{0_4}\end{bmatrix}$$

$$X_c = T_1\begin{bmatrix} X_{c_1}\\ X_{c_2}\end{bmatrix}, \qquad \dot{X}_c = T_2\begin{bmatrix} \dot{X}_{c_3}\\ \dot{X}_{c_4}\end{bmatrix} \tag{15}$$

$$X_{0_1} = X_{c_1}, \qquad \dot{X}_{0_3} = \dot{X}_{c_3} \tag{16}$$

X_{c_1} and $\dot{X}_{c_3}$ are specified by the maneuver. X_0, $\dot{X}_0$, and U_0 can now be calculated using Eqs. (7), (8), and (15). Linearizing the plant as before about X_0 and U_0, we obtain the same plant description as in Eq. (11) but with $d_x(\boldsymbol{\Theta})$ given by

$$d_x(\boldsymbol{\Theta}) = A_p(\boldsymbol{\Theta})(X_0 - X_e) + B_p(\boldsymbol{\Theta})(U_0 - U_e) + \dot{X}_e - \dot{X}_0 \quad (17)$$

and $d_y(\boldsymbol{\Theta})$ as in Eq. (12).

III. Adaptive Control Design

The problem that we address in this section is the control of the plant in Eq. (11), where A_p, B_p, d_x, and d_y are unknown, such that y_p follows y_c defined in Eq. (13). The plant can be represented in an input–output form given by

$$y_p = W_p(s)[u_p + d_0] + d_1 \quad (18)$$

where

$$W_p(s) = C(sI - A(\Theta))^{-1}B(\Theta), \qquad \in \mathbb{R}_p^{m\times m}(s) \quad (19)$$

and where d_0 is the effective input disturbance and is, therefore, canceled out using a trim error estimate added to u_p.

In Sec. III.A. the controller structure is described, after which the specific components required for its implementation on the helicopter are described in Sec.III.B. The adaptive control laws are described in Sec.III.C.

A. Controller Structure

We use a model-reference approach to determine the adaptive rules for adjusting the controllers. This requires the choice of a reference model specified by the input–output relation

$$y_m = W_m(s)r_m \quad (20)$$

One convenient and simple choice of the transfer function matrix $W_m(s)$ is given by

$$W_m(s) = R_m(s)^{-1} \quad (21)$$

where $R_m(s)$ is a polynomial matrix whose entries are monic Hurwitz polynomials. The controller structure can be described as follows[22]:

$$u_p = \Theta_c\omega(t)$$

$$\omega = \left[r_m, \omega_1^T, \ldots, \omega_{\nu-1}^T, \omega_\nu^T, \ldots, \omega_{2\nu-1}^T\right]^T$$

$$\Theta_c = [K_0, C_1, \ldots, C_{\nu-1}, D_0, \ldots, D_{\nu-1}]$$

$$\omega_i(t) = \left[s^{i-1}\big/r_q(s)\right]u(t), \qquad i = 1, \ldots, \nu - 1$$

$$\omega_j(t) = \left[s^{j-\nu}\big/r_q(s)\right]y_p(t), \qquad j = \nu, \ldots, 2\nu - 1 \quad (22)$$

C_i and D_j are chosen such that the closed-loop system has poles at desired locations. The well-known Bezout identity can be used to be determine the appropriate values of C_i and D_j as follows:

$$[(R_q - Z_c)R_p - Z_d Z_p] = R_q K_0 W_m^{-1} Z_p \quad (23)$$

$$W_p(s) = Z_p(s)R_p^{-1}(s) \quad (24)$$

$$R_q(s) = \mathrm{diag}\left(\frac{1}{r_q(s)}\right), \qquad Z_c(s) = \sum_{i=1}^{\nu-1} C_i s^{i-1}$$

$$Z_d(s) = \sum_{j=0}^{\nu-1} D_j s^j \quad (25)$$

where $Z_p(s)$ and $R_p(s)$ are in right coprime form. For the closed-loop transfer function matrix to match $W_m(s)$, we need 1) K_0 to be nonsingular and 2) $Z_p(s)$ to be stably invertible. For known values $\boldsymbol{\Theta}$, the pole-placement controller is completely specified by Eqs. (22–25). Note that, in many applications, the plant description is not readily available in the form of coprime matrices.

B. Pole Placement Control Design

As mentioned in the Introduction, the dynamic model of autonomous helicopters is given by Eqs.(1–5). These equations can then be linearized as in Eq. (11), where the nominal trim values X_0 and U_0 are to be computed for each maneuver. The controller for the plant in Eq. (11) is specified by Eqs. (22), (23), and (25). The complete control design requires the following steps to be executed: 1) Determine the nominal trim conditions X_0 and U_0, which are the solutions of Eq. (8) when $\boldsymbol{\Theta} = \boldsymbol{\Theta}_0$. 2) Determine the coprime matrices Z_p and R_p from the linearized plant parameters $A_p(\boldsymbol{\Theta}_0)$, $B_p(\boldsymbol{\Theta}_0)$, and C. 3) Ensure that the high-frequency gain K_p is nonsingular. 4) Ensure that the matrix Z_p is stably invertible. The details of steps 1-4 are given in Secs. III.B.1–III.B.4, respectively. An additional property of the relative degree of the plant model of a helicopter is outlined in Sec. III.B.5, which leads to a simple adaptive control design.

1. Determination of Nominal Trim Values X_0 and U_0

To find the trim conditions X_0 and U_0 that are the solutions of Eq. (8), 19 highly coupled nonlinear equations have to be solved, and hence, an explicit determination of the solutions X_0 and U_0 is near impossible. Optimization schemes need to be used to find a solution to this equation. Linear methods like Simplex are seen to converge to a local minima from almost all starting values. Nonlinear methods such as simulated annealing or genetic algorithms are computationally expensive. A simpler way of solving this problem is now presented that exploits insight into the nature of the helicopter dynamics and consists of a two stage optimization procedure for accurate trim determination.

Often a part of the overall state that includes the attitude angles and angular rates have either a small value for most maneuvers or values that can be determined reasonably accurately. Defining $X_a = [\phi, \theta, \psi, p, q, r]^T$, we fix $X_a = X_{ac}$, and use a simplex search to determine the remaining component X_b of X_0 and U_0. Denoting the resulting values X_1 and U_1 that this simplex search leads to, in the second stage of the nonlinear optimization, we begin with X_1 and U_1 and carry out a simplex search in the overall (X, U) space to result in the final trim determination of (X_0^*, U_0^*).

The described two-step procedure has the potential to converge to the global minimum mainly because of the prior information available about the trim values of a subcomponent of the state variables and inputs. This information is most likely available even in the most complex maneuvers, and, therefore, the procedure is a valuable step in the control design.

2. Coprime Matrix Fraction Decomposition

The next step in the control design is to find coprime matrices, $Z_p(s)$ and $R_p(s)$, starting from time-domain matrices A_p, B_p, and C, as in Eqs. (11). Diagonalizing the numerator matrix of $W_p(s)$ and separating out the poles from the transmission zeros are very sensitive to numerical errors. For the helicopter, therefore, the algorithm suggested by Bigulac and Vanlandingham[23] for right coprime matrix fraction decomposition is used. The algorithm is now briefly outlined:

1) Form selector matrices S_a, S_{ld}, and S_{li} using pseudocontrollability indices.

2) With $A_c(\Theta)$, the controllable canonical form of $A_p(\boldsymbol{\Theta})$, obtain R_{prc}, using the equations

$$R_{prc} = S_{ld} - S_{li}A_c S_a \quad (26)$$

3) Find $Z_p(s)$ using the following equations:

$$N(s) = Z_p(s)R_{p\mathrm{ad}}(s) \quad (27)$$

$$\sum_{j=0}^{i} Z_{p_j} R_{p\mathrm{ad}_{i-j}} = N_i, \qquad i = 1, \ldots, n \quad (28)$$

This algorithm is found to give a reasonably accurate representation $Z_p(s)$ and $R_p(s)$.

3. Nonsingular High-Frequency Gain

The next step is to find $Z_c(s)$ and $Z_d(s)$, using $Z_p(s)$ and $R_p(s)$ and Eq. (23). We note that a necessary requirement for finding $Z_c(s)$

and $Z_d(s)$ is the nonsingularity of K_p. In the case of the helicopter, the relative degree of some columns of $W_p(s)$ is higher than others. That is, there are some elements of the input vector $\boldsymbol{u}$ that have lower relative degree transfer functions to all outputs when compared to the other transfer functions. This results in the high-frequency gain matrix K_p to have the columns corresponding to these input elements to be identically zero. Therefore, K_p is not invertible. This problem can be resolved by filtering these input elements through stable filters of appropriate degree. A precompensator of the form

$$W_c(s) = \mathrm{diag}\left(1/\pi_p^{k_i}\right) \tag{29}$$

is selected, where k_i are equal to the maximum of the minimum column relative degree of the matrix minus the minimum column relative degree of the column i. The new input to the system v_p is given by

$$v_p = W_c(s)u_p \tag{30}$$

This changes the new transfer function of the plant to the following:

$$\bar{W}_p(s) = W_p(s)W_c(s) \tag{31}$$

We note that $\bar{W}_p(s)$ has a high-frequency gain $\bar{K}_p$ that is obviously different from K_p and is nonsingular. This enables us to find $\bar{K}_0 = \bar{K}_p^{-1}$ in the Bezout identity equation (23) corresponding to $\bar{W}_p(s)$. $\bar{K}_0$ is also nonsingular, which is needed for stable adaptation.

4. Minimum Phase Plant

To solve Eq. (23) without unstable pole-zero cancellations, we need the transmission zeros, that is, the roots of $\det Z_p(s)$, to be stable. This implies that $Z_p(s)R_p^{-1}(s)$ is minimum phase. With the input U as in Eq. (3) and output Y as in Eq. (5), we proceed to design an output $z(t) \in \mathbb{R}^5$ such that

$$z_p(t) = Ty_p(t) \tag{32}$$

where T is a postcompensator chosen such that $TZ_p(s)$ is square and has stable transmission zeros over the entire range of parameter space of interest. One natural choice of such a z_p is $z_p = [p, q, r, w, \Omega]^T$ added to other states available in Eq. (5) such that $\det Z_p(s)$ is stable. This gives us a nearly decoupled system with stable transmission zeros and no unstable pole-zero cancellations.

5. Helicopter Relative Degree

For the helicopter model, it is seen that the relative degree n_i^* of the individual elements of $W_p(s)$ is 1 or 2. This is because the relative degree of the transfer function from the thrust force to the velocity is 1 from Newton's second law. The thrust forces in turn are dependent on the angular displacement of the rotor blades. These angular displacements a_1 and b_1 are described by a relative degree-1 transfer function from the inputs U_{pcyc} and U_{rcyc}.

If the relative degree n_i^* is unity, the adaptive controller requires $m \times (2m\nu + 1)$ controller parameters and $2m\nu$ states as can be seen in Eqs. (22) because the notion of a strictly positive real transfer function can be exploited. A slight extension to the same controller structure suffices for the case when n_i^* is equal to two,[24] which requires no additional parameters, but an additional filtered output of ω. The number of states and parameters in both cases are significantly smaller than those in the case when n_i^* is greater than two. For a plant with $m = 5$ and $\nu = 4$, the controller states are 80 when $n_i^* = 2$ in comparison to 440 when $n_i^* = 3$.

The complete system is now represented by the following equation:

$$z_p = TZ_p(s)R_p^{-1}(s)W_c(s)[u_p + d_0(\boldsymbol{\Theta})] + Td_1(\boldsymbol{\Theta}) \tag{33}$$

Here $Z_p(s)R_p^{-1}(s)$ is the coprime matrix fraction decomposition of the state-space model in Eq. (11). The output in Eq. (5) is assumed to have all available states.

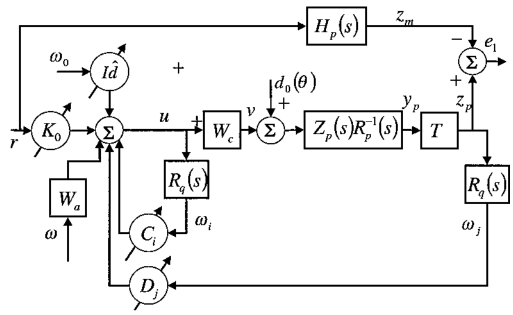

Fig. 2 Multivariable plant with the proposed adaptive controller.

C. Adaptive Pole-Placement Control

The adaptive controller is now designed for the partial state feedback case of the helicopter. The system is described by Eq. (11), and with the addition of the precompensator and postcompensator, the transfer function changes to the representation in Eq. (33). An adaptive controller structure based on the structure in pole-placement controller described before is now chosen for the helicopter (Fig. 2). To compensate for d_0 in Eq. (18), ω and Θ_c are augmented as $\bar{\omega} = [\omega_0^T, \omega^T]^T$ and $\bar{\Theta}_c(t) = [\hat{d}^T(t), \Theta_c^T(t)]^T$, which results in the controller

$$u_p(t) = \bar{\Theta}_c(t)\bar{\omega}(t) \tag{34}$$

We define $\bar{\Theta}_c^*$ as the constant value of the controller parameters for which the closed-loop transfer function satisfies $W_{\mathrm{cl}}(s) \equiv H_p(s)$. $H_p(s)$ is the hermite normal form of the plant in Eq. (33) and is diagonal.[24] The error, $e_1(t) = z_p(t) - z_m(t)$, is derived as

$$e_1(t) = H_p(s)K_p\Phi(t)\bar{\omega}(t) + Td_1(\boldsymbol{\Theta}) \tag{35}$$

where $\Phi(t) = \bar{\Theta}_c(t) - \bar{\Theta}_c^*$ and z_m is the output of the reference plant

$$z_m(s) = H_p(s)r_m \tag{36}$$

For stable adaptation the transfer function $H_p(s)$ needs to be strictly positive real (SPR). If the elements of $H_p(s)$ are of relative degree 2, the input and error equations are modified as

$$u(t) = \dot{\bar{\Theta}}_c(t)W_a(s)\bar{\omega}(t) + \bar{\Theta}_c(t)\bar{\omega}(t) \tag{37}$$

$$e_1(t) = H_p(s)W_a^{-1}(s)K_p\Phi(t)\omega(t) + Td_1(\boldsymbol{\Theta}) \tag{38}$$

where

$$W_a(s) = [1/(s+a)]I, \qquad a > 0 \tag{39}$$

and are chosen such that $H_p(s)W_a(s)$ is SPR.[24] The following adaptation law is now chosen for stable adaptation:

$$\dot{\bar{\Theta}}_c = -Pe_1W_a(s)\bar{\omega}^T - \Gamma_r\bar{\Theta}_c, \qquad \Gamma_r > 0 \tag{40}$$

$$P = \Gamma^{-1} \tag{41}$$

where

$$\Gamma K_p + K_p^T\Gamma = Q_0 > 0, \qquad \forall\boldsymbol{\Theta} \in \Theta_s \tag{42}$$

Γ_r is chosen for robustness of the design to the trim disturbance $d_1(\boldsymbol{\Theta})$, nonlinearities, noise, and other disturbances.

The initial value of K_0 is the inverse of K_p^{-1}, for the plant in Eq. (33) with nominal values for $\boldsymbol{\Theta}$. The initial value of $\hat{d}$ is chosen as zero. The initial values of the rest of the controller parameters Θ_c are found by solving Eq. (23) with W_m replaced by H_p, that is, by solving

$$[(R_q - Z_c)R_p - Z_dZ_p] = R_qK_0H_p^{-1}Z_p \tag{43}$$

Theorem: For the plant given in Eq. (33), model in Eq. (36), and controller given in Eq. (37), given an $H_p(s)W_a(s)$ that is SPR and a K_p that satisfies Eq. (42), the adaptation law in Eqs. (40) and (41) guarantees that all signals of the closed-loop system are bounded.

The reader is referred to Narendra and Annaswamy[24] for the proof.

Table 1 Summary of numerical simulation tasks

Task	Advantages of adaptive controller	Figures
1) Step changes in forward velocity	Low steady-state error, improvement in transients over time, little overshoot, good learned performance after adaptation is stopped.	3–5
2) Sinusoidal forward velocity command	Low steady-state error, low transients, good learned performance after adaptation is stopped for frequencies different from training set.	7, 8
3) Step changes in vertical velocity	Low steady-state error, low transients, and improvement in transients over time, little overshoot, good learned performance	9, 10
4) Coordinated turn	Low transients, smaller tracking error, good learned performance	11, 12

IV. Numerical Studies

The controller presented in the preceding section is simulated for the nonlinear dynamics presented in Sec. II.A. The uncertainties used are 2% and 20% increases in m and I_{yy}. These parameters are seen to have the worst impact on the stability of the system, and an increase in their values is seen to have the most effect. Four different tasks are performed, and the results of the dynamic inversion controllers are compared against the adaptive controller. Adaptation is stopped after a time in each case based on the output error value to observe learning behavior of the controller. The results are summarized in Table 1.

The simulations use a high-fidelity model of the helicopter including aerodynamics and thrust calculations as described by Johnson and DeBitetto.[21] However, for tasks 1 and 2, the model is simplified to only the longitudinal dynamics and with the actuator dynamics neglected. The complete model with actuator dynamics is used for tasks 3 and 4. Because this study represents a first step in the design of a truly autonomous helicopter, the saturation constraints on the inputs have not been incorporated. The proposed controller is demonstrated in comparison with other existing controllers designed with the same assumptions.

A. Controllers for Comparison

We use three fixed controllers based on linear quadratic (LQ) method,[9] dynamic inversion (DI),[12] and integrator-based design,[9] whose performances will be compared to the adaptive controller presented in this paper.

B. Task 1: Track Step Changes in Forward Flight Velocity

The first simulation involves step changes in forward flight velocity between 28 and 40 ft/s for the helicopter. (Higher speeds can be achieved with this controller by gain scheduling. We also note that tasks 3 and 4 address more complex maneuvers where gain scheduling was used successfully. For ease of exposition, the speed was limited to 40 ft/s. Note that this speed is significantly larger than what was previously studied in the Charles Stark Draper Laboratory simulation studies.[21]) In this maneuver, random steps are taken subsequent to the stoppage of adaptation to test the learned behavior of the adaptive controller. The LQ controller, designed without the inclusion of aerodynamics and assuming full state access, is compared against the adaptive controller. Because in this case all relevant states are accessible, a simpler adaptive controller of the form

$$u_p = Q(Kx_p + r_m + \hat{d}) \tag{44}$$

$$\dot{K} = -\Gamma_1\left[B_m^T P e x_p^T + \Gamma_{r1} K\right] \tag{45}$$

$$\dot{Q} = -\Gamma_2\left[Q B_m^T P e u_p^T Q - \Gamma_{r2} Q\right] \tag{46}$$

$$\dot{\hat{d}} = -\Gamma_3\left[B_m^T P e + \Gamma_{r3}\hat{d}\right] \tag{47}$$

was used, whose details can be found by Krupadanam.[25] The LQ controller has the same structure as in Eq. (44), where Q and K are fixed at values that minimize a suitable quadratic cost function and $\hat{d}$ set to zero.

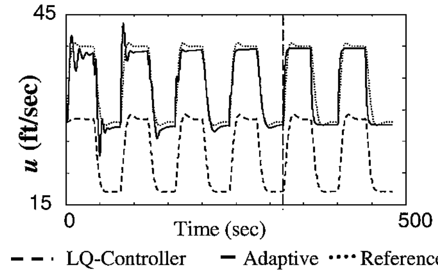

Fig. 3 Comparison of adaptive and linear LQ controllers in task 1; step changes in forward flight velocity.

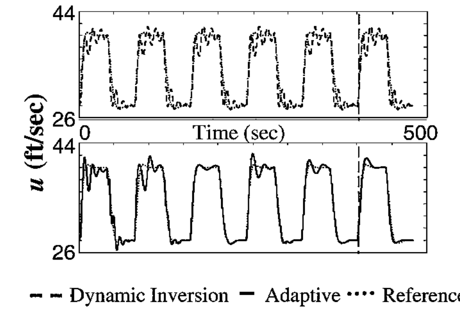

Fig. 4 Comparison of adaptive and linear DI controllers in task 1; step changes in forward flight velocity: responses of u vs time shown from 0–500 s, with adaptation stopped at 400 s.

Figure 3 compares the adaptive controller against the LQ controller with aerodynamics included in the system design. It can be seen that the LQ controller has a large steady-state bias. This is because the nonlinear part of the dynamics due to the aerodynamics are neglected in the design. The response of a reference model is also included in Fig. 3, where the reference model corresponds to the nominal linearized dynamics of the plant with the LQ controller. The adaptive controller was chosen as in Eqs. (44–47) but with $\hat{d}$ fixed as zero, and with the starting values for K and Q as those for the LQ controller. As shown in Fig. 3, the steady-state bias is reduced by as much as 95% in the adaptive case. The resulting responses of u vs time are shown from 0 to 500 s, with adaption stopped at 320 s. As shown in Fig. 3, even though adaptation was stopped at 320 s, the adaptive controller continues to outperform the LQ controller.

To address the issue of steady-state bias, an integral action was added to the DI controller, and the $\hat{d}$ term was adjusted as in Eq. (47) of the adaptive controller. The resulting response is shown in Fig. 4. The adaptive controller is chosen as in Eqs. (44–47) with the trim estimate $\hat{d}$. DI reduces the steady-state bias compared to the LQ controller. The addition of integrators eliminates steady-state error but increases transients for the DI controller. For example, for a control design that maintains a rise time of less than 5 s, transients of magnitude upto 10% of the step size and settling time greater than 40 s are introduced with integral action. In contrast, the adaptive controller is seen to outperform this controller by having low steady-state bias, fast rise time, and no overshoot or transients after the initial adaptation. The initial transients introduced by the adaptation are of similar magnitude as those of the DI controller with integrators. These are eliminated in subsequent iterations of the maneuver as the controller parameter errors decrease. Finally, even after the adaptation is stopped, the controlled system continues to show the learned performance.

Figure 5 shows training of the adaptive controller for a series of steps followed by stoppage of adaptation. The adaptive controller is chosen as before. The DI controller includes an integrating action. Random steps are then taken in forward velocity with the same controller values. This shows that the controller gains and trim error estimate learned in the initial series of constant steps is sufficient to provide good performance for maneuvers of similar frequency content. This is because the adaptation enables the controller to

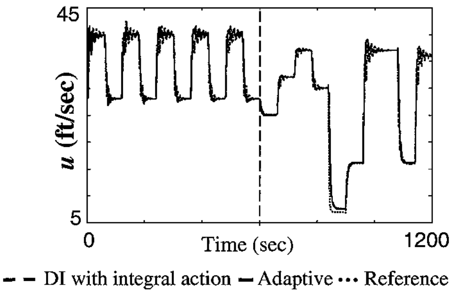

Fig. 5 Comparison of adaptive and linear DI controllers in task 1 for random step changes in forward flight velocity after a certain time: responses of u vs time shown from 0 to 1200 s, with adaptation stopped at 600 s.

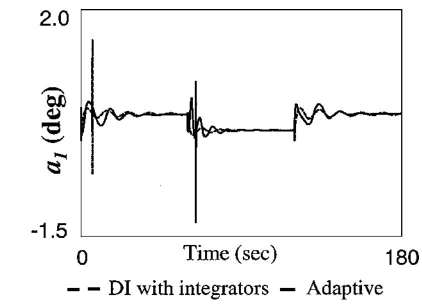

Fig. 6 Comparison of adaptive and linear DI controllers in task 1 for step changes in forward flight velocity: a_1 vs time.

minimize the state error for the particular maneuver. The controller gains are, therefore, values that make the adapted system similar to the reference model for these frequencies.

The main rotor pitch flapping angle a_1 is shown in Fig. 6 for the first 180 s, which corresponds to three initial steps in forward velocity. It is seen that the bandwidth requirements are similar for the adaptive and DI controller in the first two steps. The maximum required magnitude and angular rates for a_1 are around 7 and 65 s for the DI controller and adaptive controller, respectively. From the third step onward the bandwidth requirements are lower for both cases, as seen from the transients. The maximum main rotor flapping angular rate is less than 10 deg/s for both the adaptive and the DI controller. Thus, the adaptive controller achieves better performance in the long run without any greater bandwidth requirements on the inputs.

C. Task 2: Complex Maneuver in Forward and Vertical Velocities

We now a consider a maneuver that is to jump over hurdles, that is, to track a circle in the U_g–W_g plane. Because the commanded velocities vary significantly, a gain-scheduled approach is used with 12 distinct operating points along the maneuver, both for the adaptive and the DI controllers. The DI controller is designed as in task 1, with integrators. The adaptive controller as in Eqs. (44–47) in task 1 is used with trim estimate $\hat{d}$. The resulting performances are shown in Figs. 7 and 8. The responses of U_g vs W_g are shown over the first cycle (Fig. 7) and eight cycle (Fig. 8). The DI controller is seen to have very large initial transients, and with time, the integral action reduces the tracking error. In contrast, the adaptive controller results in smaller transients (Fig. 7) and in an even smaller tracking error (Fig. 8).

D. Task 3: Vertical Flight with Partial State Access

The controller presented in Sec. III is now simulated for the full helicopter dynamics presented in Sec. II.A with a 20% uncertainty in the mass. The task performed involves steps in vertical velocity that varies between 5 and 10 ft/s. The resulting sysem has four inputs and four outputs with the throttle kept constant. The states that are not accessible are a_1, b_1, $a_{1,\mathrm{FB}}$, $b_{1,\mathrm{FB}}$ and λ_f. The results of the adaptive controller are compared with a pole-placement controller of a similar structure but with fixed parameters, which are 96 in number. Adaptation is stopped in the former case, after a certain time as in tasks 1 and 2, to observe learning. Note that the adaptive controller design includes, as initial values for the control parameters, plant

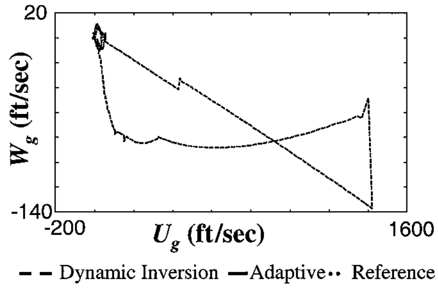

Fig. 7 Comparison of adaptive and linear DI controllers in task 2; a circle in the U_g–W_g plane; response over first cycle.

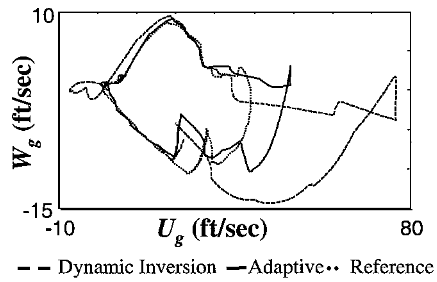

Fig. 8 Comparison of adaptive and linear DI controllers in task 2; a circle in the U_g–W_g plane; response over eighth cycle.

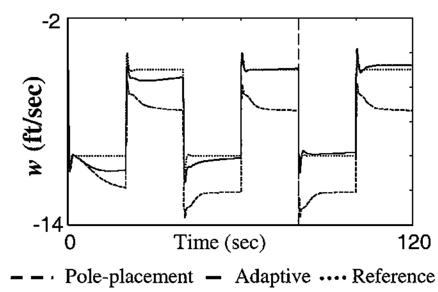

Fig. 9 Comparison of adaptive and linear pole-placement controllers in task 3; steps in vertical flight: responses of w vs time for 0–120 s, with adaptation stopped at 80 s.

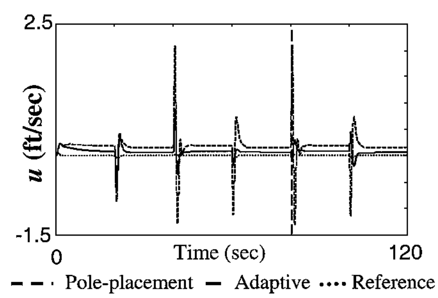

Fig. 10 Comparison of adaptive and linear pole-placement controllers in task 3; steps in vertical flight: responses of u vs time for 0–120 s, with adaptation stopped at 80 s.

parameters obtained with linearization around nominal parameter values with the aerodynamics included. At these speeds, a design that neglects aerodynamics has inadequate robustness properties and invariably, simulations fail because of unacceptably large transients.

The resulting performances of the controllers in the states w and u are shown in Figs. 9 and 10, which shows that the adaptive controller outperforms the pole-placement controller in terms of steady-state error and transients. In the case of the forward velocity, the transients are seen to be lower than the pole-placement controller. Figures 9 and 10 also show that the adaptive controller exhibits a suitable learning behavior; even though the adaptation is switched off after just two cycles, the tracking performance is seen to be as good as in the last adaptive cycle. The adaptive controller also eliminates the steady-state bias.

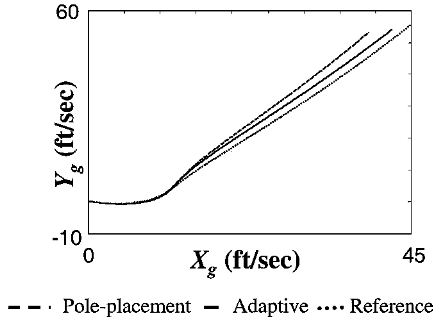

Fig. 11 Comparison of adaptive and linear pole-placement controllers in task 4; coordinated turn: responses of X_g vs Y_g over the first cycle.

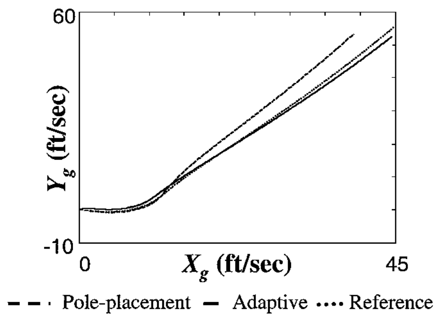

Fig. 12 Comparison of adaptive and linear pole-placement controllers in task 4; coordinated turn: responses of X_g vs Y_g after adaptation has been stopped.

E. Task 4: Coordinated Turn

In this maneuver, the helicopter moves from a coordinated turn of from 2.5 to 5 deg/s with a forward velocity of 5 ft/s. A 20% uncertainty in the mass is added to the system. The requisite controller in this case has 200 parameters. As in task 4, we compare the performance of the adaptive controller with a pole-placement controller of a similar structure. In this case, too, the adaptive controller is seen to outperform the pole-placement controller (Fig. 11). In this maneuver, over a period of 30 s the linear controller is seen to result in a 6.5-ft error in the displacement of the helicopter from the nominal designed model. The helicopter travels about 45 ft in the X_g direction during this period. The adaptive controller reduces the error to less than 3 ft in the first cycle and to around 2 ft in the second cycle. In addition to the reduction in the steady-state error, the transients are reduced with time. Moreover, after stoppage of adaptation, it was observed the learned values of controller parameters continue to show good performance for the maneuver (Fig. 12).

V. Conclusions

This paper provides a design procedure for the multivariable adaptive control of an autonomous helicopter. In the design model, all typically present aerodynamics, parametric uncertainties, and trim error are included. The adaptive controller includes a trim error estimate and provides for stable adaptation even in the presence of nonminimum phase helicopter dynamics. The controllers are demonstrated through simulations for the control of an autonomous helicopter for maneuvers involving trajectory tracking, steady-state bias, and complex maneuvers and show considerable improvement with adaptation. The adaptive controller is stable, is robust, and shows significant improvement in performance over other control designs. This new methodology is a control design tool that helps bridge the gap between multivariable adaptive control theory and the needs of realistic applications such as autonomous helicopters.

Acknowledgments

This work was sponsored by Charles Stark Draper Laboratory University Research and Development Grant 902. The authors thank the Associate Editor, S. Osder, and the anonymous reviewers for their comments and suggestions, which helped place the contributions of the paper in proper perspective.

References

[1]Prouty, R. W., *Helicopter, Performance, Stability, and Control*, Krieger, Malabar, FL, 1990.

[2]Tischler, M. B., "Assessment of Digital Flight-Control Technology for Advanced Combat Rotorcraft," *Journal of the American Helicopter Society*, Vol. 34, No. 4, 1989, pp. 66–76.

[3]Tischler, M. B., Fletcher, J. W., Morris, P. M., and Tucker, G. E., "Flying Quality Analysis and Flight Evaluation of a Highly Augmented Combat Rotorcraft," *Journal of Guidance, Control, and Dynamics*, Vol. 14, No. 5, 1991, pp. 954–963.

[4]Osder, S., and Caldwell, D., "Design and Robustness Issues for Highly Augmented Helicopter Controls," *Journal of Guidance, Control, and Dynamics*, Vol. 15, No. 6, 1992, pp. 1375–1380.

[5]Postlethwaite, I., Smerlas, A., Walker, D. J., Gubbels, A. W., Baillie, S. W., Strange, M. E., and Howitt, J., "H_∞ Control of the NRC Bell 205 Fly-by-Wire Helicopter," *Journal of the American Helicopter Society*, Vol. 44, No. 4, 1999, pp. 276–284.

[6]Ekblad, M., "Reduced-Order Modeling and Controller Design for a High-Performance Helicopter," *Journal of Guidance, Control, and Dynamics*, Vol. 13, No. 3, 1990, pp. 439–449.

[7]Hess, R. A., and Gorder, P. J., "Quantitative Feedback Theory Applied to the Design of a Rotorcraft Flight Control System," *Journal of Guidance, Control, and Dynamics*, Vol. 16, No. 4, 1993, pp. 748–753.

[8]Low, E., and Garrard, W. L., "Design of Flight Control Systems to Meet Rotorcraft Handling Qualities Specifications," *Journal of Guidance, Control, and Dynamics*, Vol. 16, No. 1, 1993, pp. 69–78.

[9]Shim, D. H., Koo, T. J., Hoffmann, F., and Sastry, S., "A Comprehensive Study of Control Design for an Autonomous Helicopter," *37th Institute of Electronics and Electrical Engineers Conference on Decision and Control*, IEEE Publ., Piscataway, NJ, 1998, pp. 3653–3658.

[10]Dudgeon, G. J. W., and Gribble, J. J., "Helicopter Attitude Command Attitude Hold Using Individual Channel Analysis and Design," *Journal of Guidance, Control, and Dynamics*, Vol. 20, No. 5, 1997, pp. 962–971.

[11]Rozak, J. N., and Ray, A., "Robust Multivariable Control of Rotorcraft in Forward Flight: Impact of Bandwidth on Fatigue Life," *Journal of the American Helicopter Society*, Vol. 43, No. 7, 1998, pp. 195–201.

[12]Snell, S. A., and Stout, P. W., "Robust Longitudinal Control Design Using Dynamic Inversion and Quantitative Feedback Theory," *Journal of Guidance, Control, and Dynamics*, Vol. 20, No. 5, 1997, pp. 933–940.

[13]Prasad, J. V. R., Calise, A. J., Corban, J. E., and Pei, Y., "Adaptive Nonlinear Controller Synthesis and Flight Test Evaluation on an Unmanned Helicopter," *Institute of Electronics and Electrical Engineers Conference on Control Applications*, Vol. 1, IEEE Publ., Piscataway, NJ, 1999, pp. 137–142.

[14]Sanders, C. P., DeBitetto, P. A., Feron, E., Vuong, H. F., and Leveson, N., "Hierarchical Control of Small Autonomous Helicopters," *37th Institute of Electronics and Electrical Engineers Conference on Decision and Control*, IEEE Publ., Piscataway, NJ, 1998, pp. 3629–3634.

[15]Frazzoli, E., Dahleh, M. A., and Feron, E., "Robust Hybrid Control for Autonomnous Vehicle Motion Planning," *39th Institute of Electronics and Electrical Engineers Conference on Decision and Control*, IEEE Publ., Piscataway, NJ, 2000, pp. 821–826.

[16]Koo, T. J., and Sastry, S., "Differential Flatness Based Full Authority Helicopter Control Design," *38th Institute of Electronics and Electrical Engineers Conference on Decision and Control*, IEEE Publ., Piscataway, NJ, 1999, pp. 1982–1987.

[17]Frazzoli, E., Dahleh, M. A., and Feron, E., "Trajectory Tracking Control Design for Autonomous Helicopters Using a Backstepping Algorithm," *American Control Conference*, American Control Conf., Chicago, IL, 2000, pp. 4102–4107.

[18]Junkins, J. L., and Akella, M. R., "Nonlinear Adaptive Control of Spacecraft Maneuvers," *Journal of Guidance, Control, and Dynamics*, Vol. 20, No. 6, 1997, pp. 1104–1110.

[19]Stepniewsky, W. Z., and Keys, C. N., *Rotary-Wing Aerodynamics*, Dover, New York, 1984.

[20]Heffley, R. K., and Mnich, M. A., "Minimum-Complexity Helicopter Simulation Math Model," NASA CR-177476, NASA Ames Research Center, Moffett Field, CA, 1988.

[21]Johnson, E. N., and DeBitetto, P. A., "Modeling and Simulation for Small Autonomous Helicopter Development," AIAA Paper 97-3516, AIAA, Reston, VA, 1997, pp. 1997–3511.

[22]Singh, R. P., "Stable Multivariable Adaptive Control Systems," Ph.D. Dissertation, Dept. of Electrical Engineering, Yale Univ., New Haven, CT, May 1985.

[23]Bigulac, S., and Vanlandingham, H. F., *Algorithms for Computer-Aided Design of Multivariable Control Systems*, Marcel Dekker, New York, 1993.

[24]Narendra, K. S., and Annaswamy, A. M., *Stable Adaptive Systems*, Prentice–Hall, Englewood Cliffs, NJ, 1989.

[25]Krupadanam, A. S., "A Viable Multivariable Adaptive Controller with Application to Autonomous Helicopters," Ph.D. Dissertation, Dept. of Mechanical Engineering, Massachusetts Inst. of Technology, Cambridge, MA, July 2001.